Supplementary Information

Aggregation between oligomeric Ir photosensitizers promote efficient and long-lifetime photocatalytic hydrogen evolution

Yifan Huang,[a,b] Shihan Liu,[a,b] Bo Wang,[c] Ying Wang,*[b,d] Yifan Zhang*[a,b] and Pengyang Deng*[a,b]

1. Materials

$IrCl_3 \cdot xH_2O$ (≥ 98.0%). 2-phenylpyridine (ppy, ≥ 98.0%), 3,3',4,4'-Biphenyl tetracarboxylic diandhydride (BPDA, ≥ 98.0%), and hydroquinone diphthalic anhydride (HQDA, ≥ 98.0%) are purchased from Bidepharm Corporation. 1,4,5,8-naphthalenetetracarboxylic dianhydride (NPTA) is purchased from Tokyo Chemical Industry (TCI). 4,4′-Oxydiphthalic anhydride (ODPA) is purchased from Shanghai Macklin Biochemical Co., Ltd. 4,4'-diamino-2,2'-bipyridyl (dabpy, ≥ 98.0%), NH_4PF_6 (≥ 98.0%), N, N-Dimethylformamide (DMF) (99.8%, Extra Dry), dimethyl-acetamide (DMAc) (99.8%, Extra Dry) and Triethylamine (TEA, ≥ 99.9%) are purchased from Energy Chemical Corporation. Ethanol (A.R.), methanol (A.R.), petroleum ether (A.R.), ethyl acetate (A.R.), dichloromethane (A.R.), dimethylformamide (DMF) (A.R.), and HNO_3 (65-68%, A.R.) are purchased from Xilong Scientific Corporation. Potassium platinochloride (K_2PtCl_4, ≥ 99.9%) is purchased from Sigma Aldrich Corporation. All starting materials required no further purification. Deionized water is used throughout all experiments.

2. DFT calculation software and calculation method

All the calculations for the studied complexes were performed using the Gaussian 09 program package.[1] Density functional theory calculations (DFT) [2] were carried out using Becke's three parameter nonlocal exchange functional[3] with the gradient correction of the Lee, Yang, and Parr[4] (B3LYP) together with LANL2DZ basis set[5,6].

3. Further analysis of H4 and H5 photocatalytic performance

First, H4 has the best stability, but its initial rate of hydrogen evolution is lower than that of H1-3. This phenomenon could be explained by the following aspects: (i) the Ir complex H1 does not have linkers, the diffusion of the catalysts, sacrificial agents and solvent molecules to the active site of H1 is easy; (ii) the rigid linker of H2-3 are not easily deformable, which only slightly hindrance the diffusion of catalysts, sacrificial agents and solvent molecules to the active site; (iii) the flexible linkers of H4 tend to distort and fold, causing a relatively larger hindrance to diffusion of catalysts, sacrificial agents and solvent molecules to the active site of H4, resulting in a relatively lower initial hydrogen evolution rate of H4.

Second, H5 exhibits a lower photocatalytic and a lower stability than H4. The reason is as follows: (i) according to the DFT calculations, the vertical crossover conformation of aggregated H5 has much larger energy gaps than all the presented conformations of H2-4, and the crossover conformation of aggregated H5 is relatively stable. The vertical crossover conformation in aggregated H5 will show lower electron transfer ability than other conformations, which may affect the photocatalytic activity of aggregated H5; (ii)

the relatively lower stability of H5 is possibly due to the longer flexible linker on auxiliary ligands leading to more structure distortion, the structure distortion exerts extra force on the auxiliary ligands and slightly reduces the stability of H5.

4. Detailed liquid UV absorption spectrum analysis

In order to determine the UV-Vis spectra and band gap variations of H1-H5 in the presence of near single molecule dispersion, liquid UV-Vis absorption spectra were characterized. Liquid UV weighing ~0.001 g of solid was dissolved in 10 mL of DMF /H_2O/TEA (3/1/1,v/v/v) solvent, sonicated to fully dissolve the imine, and then diluted at 1/4 and 1/10 ratios and tested after dilution. 1/4 dilution conditions resulted in energy gaps of H1-H5 in the following order: 3.84 eV, 3.67 eV, 3.69 eV, 3.67 eV, and 3.69 eV. The energy gaps of H1-H5 at 1/10 dilution were in the following order: 3.87 eV, 3.72 eV, 3.75 eV, 3.72 eV, and 3.72 eV. According to the test results, H3 exhibited the weakest light absorption intensity due to the lowest solubility, while H2, H4, and H5 had essentially the same absorption intensity. the band gap widths of H2-H5 were essentially the same, but show a pattern of variation close to that calculated by DFT and are all lower than H1. This is a side indication that the band gap changes significantly in the monodisperse case compared to the pure solid.

To further exclude the effect of possible hydrogen bonding of water with imines on the results, liquid UV-Vis absorption spectra of H1-H5 were characterized with DMF/TEA (3/1, v/v) as the solvent. The energy gaps of H1-H5 at 1/4 dilution were in the order of 3.79 eV, 3.61 eV, 3.72 eV, 3.65 eV, and 3.67 eV. At 1/10 dilution, the energy gaps of H1-H5 were in the order of 3.72 eV, 3.68 eV, 3.65 eV, 3.56 eV and 3.68 eV. According

to the test H3 also exhibits the weakest light absorption intensity and the band gap widths of H2-H5 are essentially the same. At the same time, H2-H5 exhibits the same results as the calculated DFT in the bimolecular state under 1/4 dilution conditions. Such results indicate that the agglomeration state has a significant influence on the energy band structure of the imine oligomer molecules.

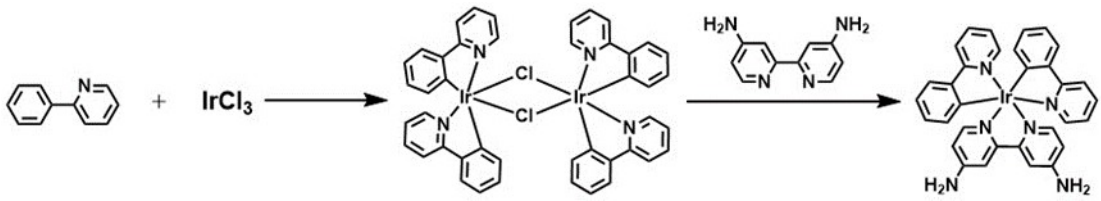

Figure S 1 The synthesis process of $Ir(ppy)_2(dabpy)$ (H1).

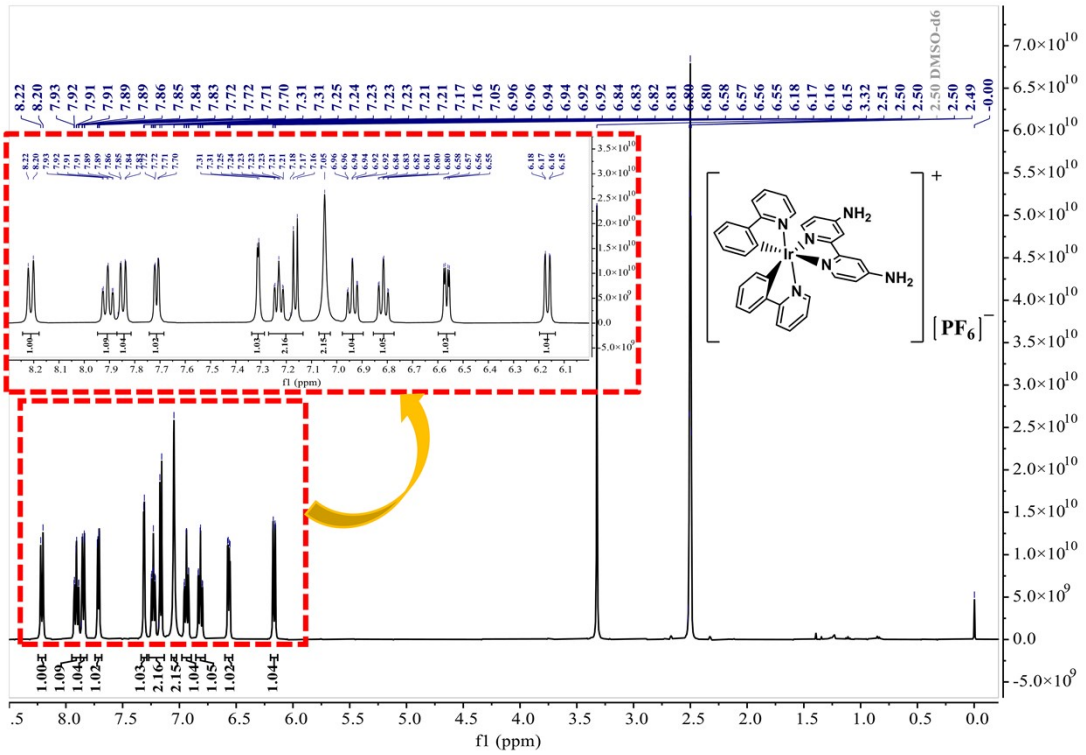

Figure S 2 The ^1H NMR of H1. The insets show enlargements of the characteristic regions and the molecular structure.

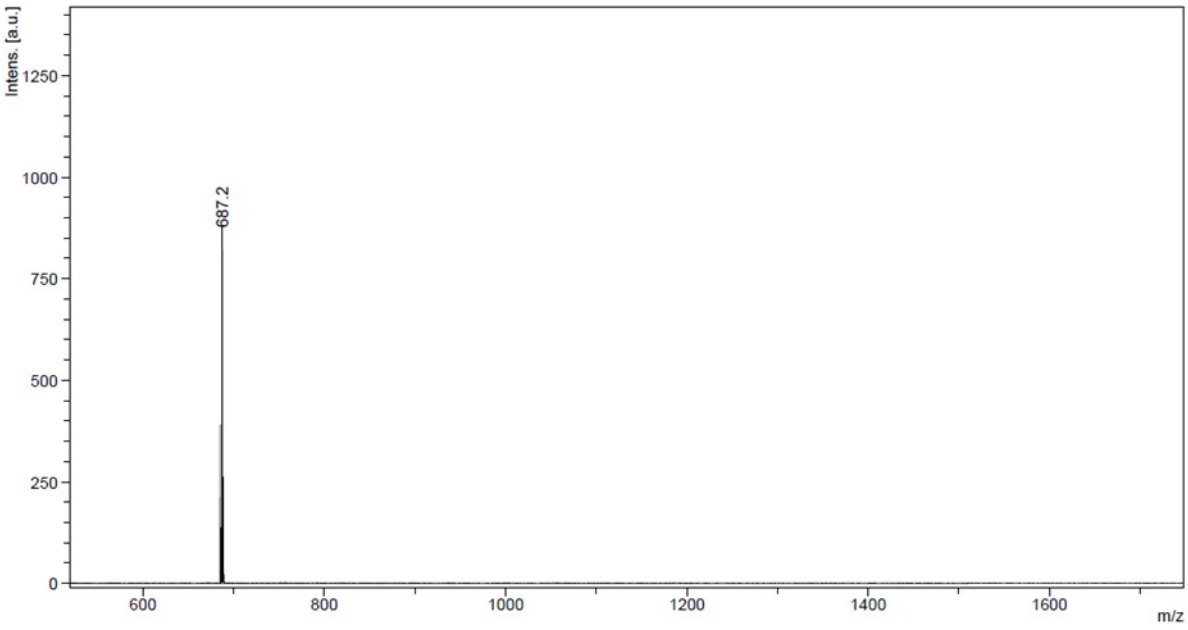

Figure S 3 The MALDI-TOF MS of H1.

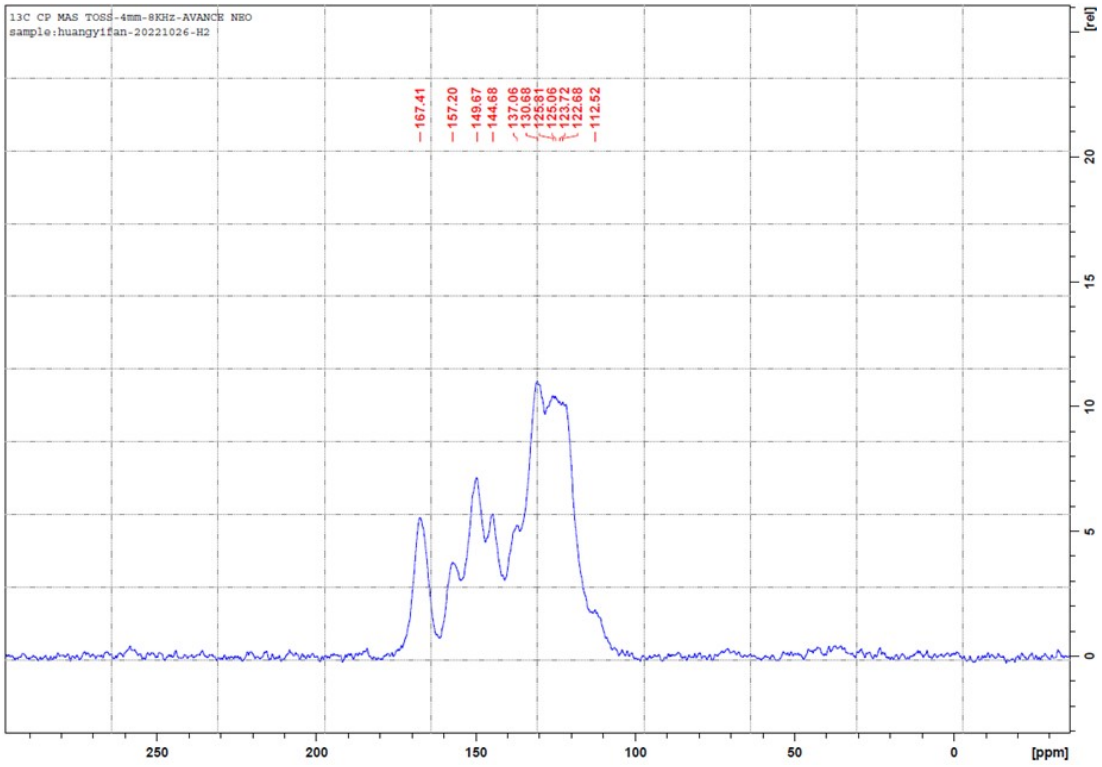

Figure S 4 The solid-state NMR of H2.

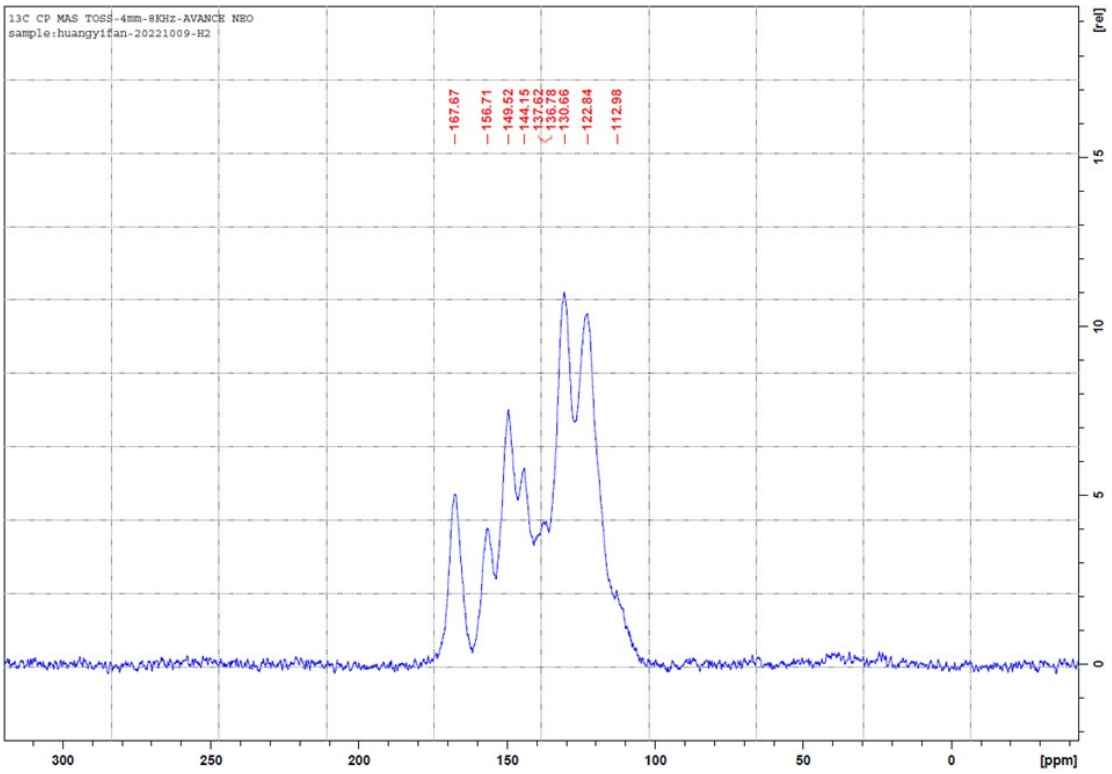

Figure S 5 The solid-state NMR of H3.

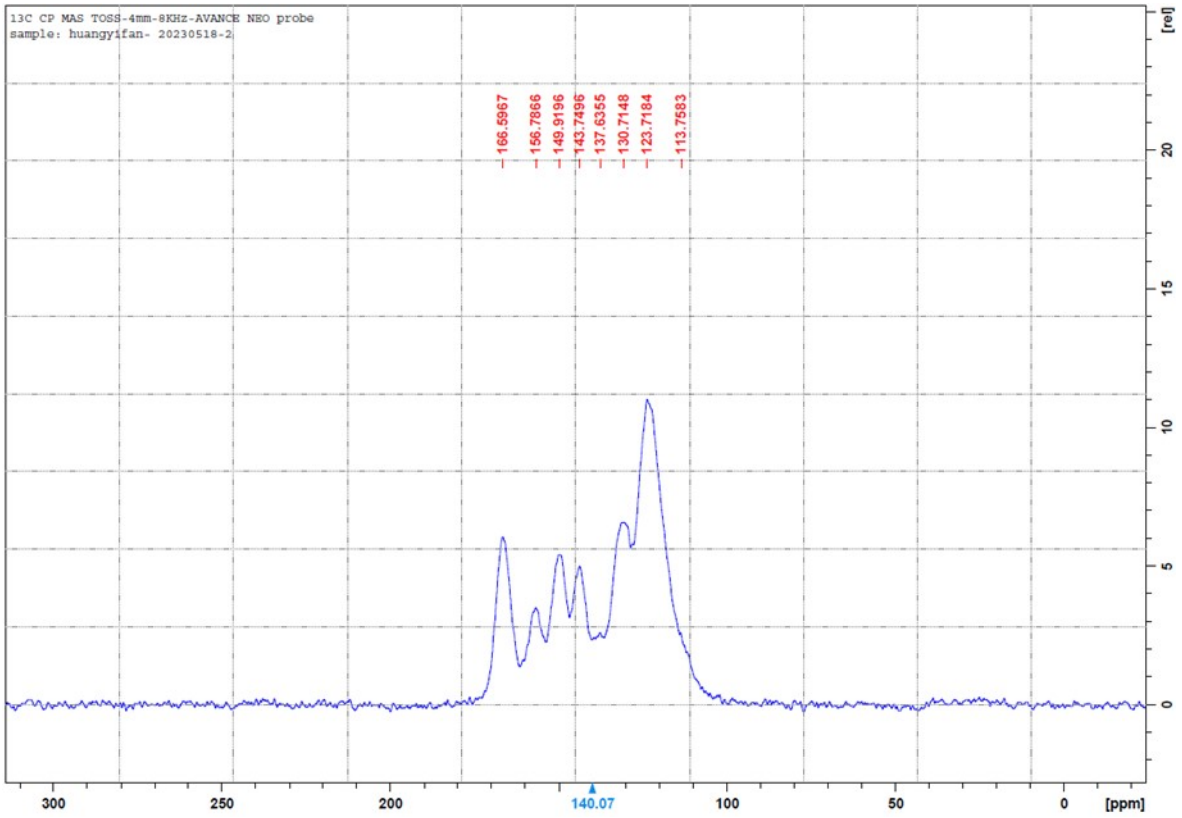

Figure S 6 The solid-state NMR of H4.

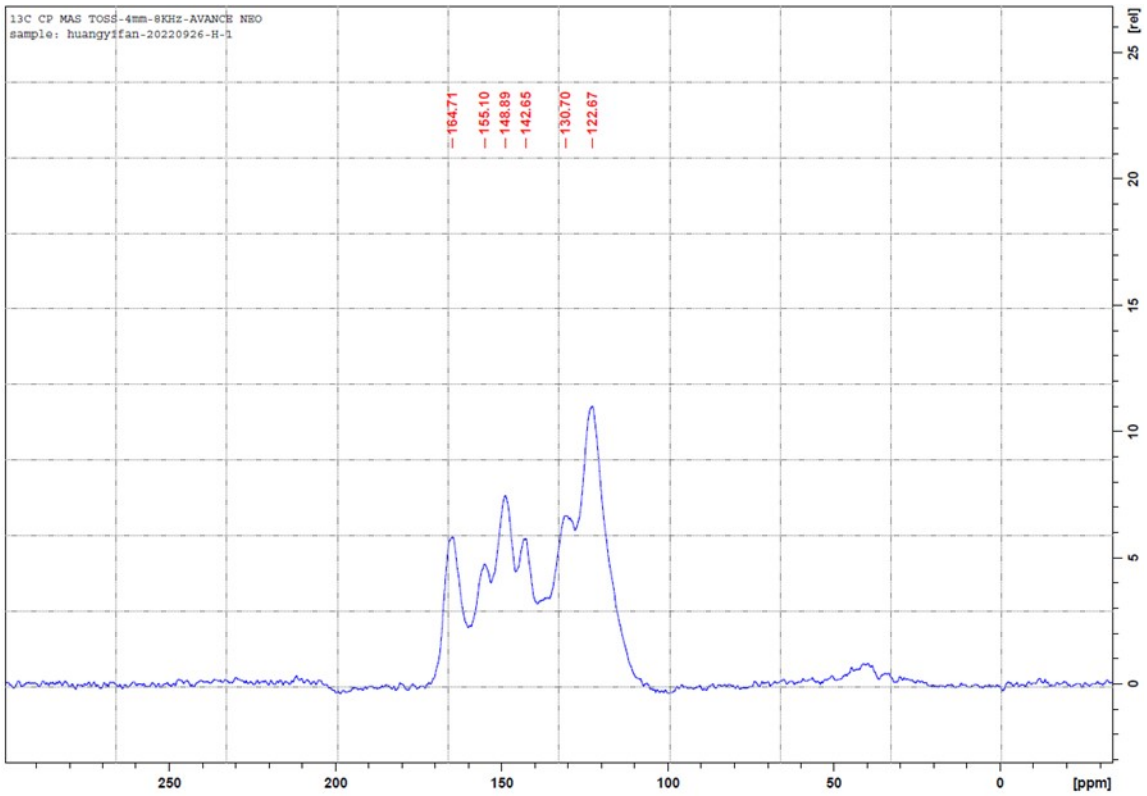

Figure S 7 The solid-state NMR of H5.

Table S 1 The binding energy corresponding to each peak position of XPS N1s.

	Pyridine N (eV)	Amino N (eV)	Imine N (eV)
H1	399.80	400.25	/
H2	399.85	400.30	401.25
H3	399.95	400.40	401.45
H4	400.00	400.45	401.45
H5	400.05	400.45	401.50

Table S 2 The binding energy corresponding to each peak position of XPS Ir 4f.

	Ir $4f_{5/2}$ (eV)	Ir $4f_{7/2}$ (eV)

H1	64.75	61.70
H2	64.55	61.60
H3	64.70	61.70
H4	64.55	61.60
H5	64.65	61.65

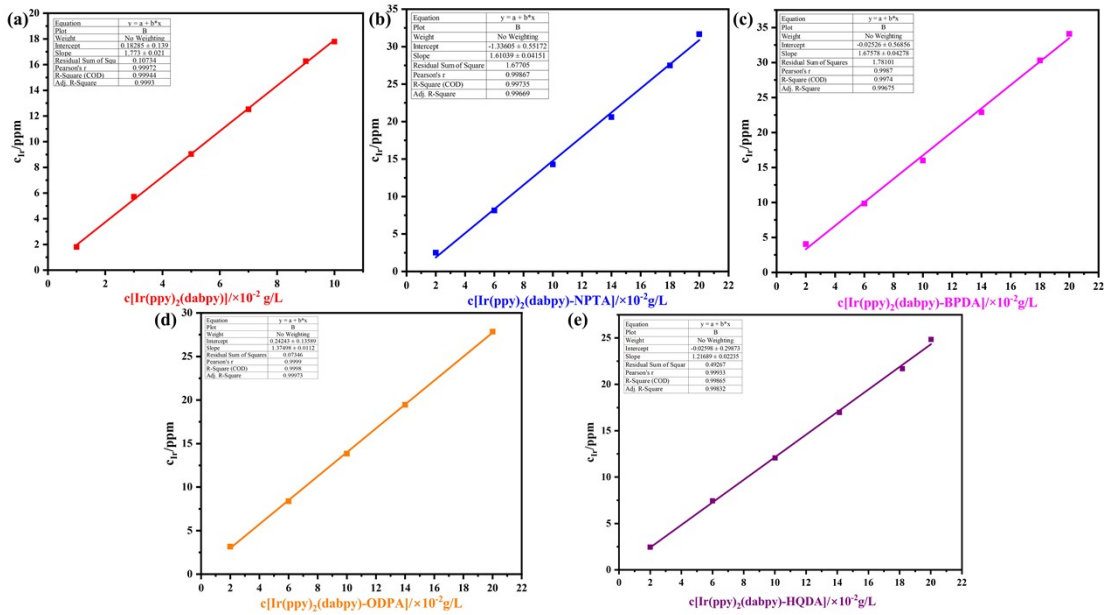

Figure S 8 H1-H5 ablation calibration curve.

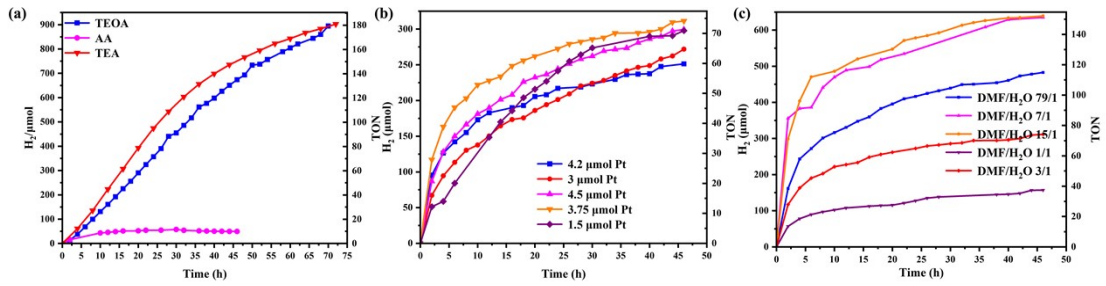

Figure S 9 Optimization of photocatalytic conditions for H4 (a) Photocatalytic performance of H4 under different sacrificial agent conditions. (b) The photocatalytic performance of H4 under different Pt concentrations. (c) The photocatalytic performance of H4 under different solvent-to-water ratios.

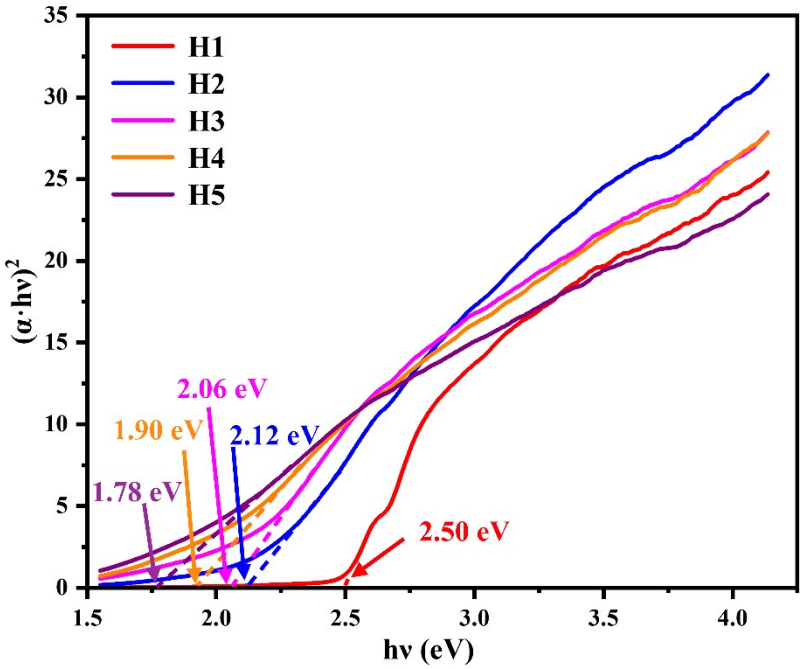

Figure S 10 H1-H5 UV absorption spectra calculated from Tauc plots of the energy gaps.

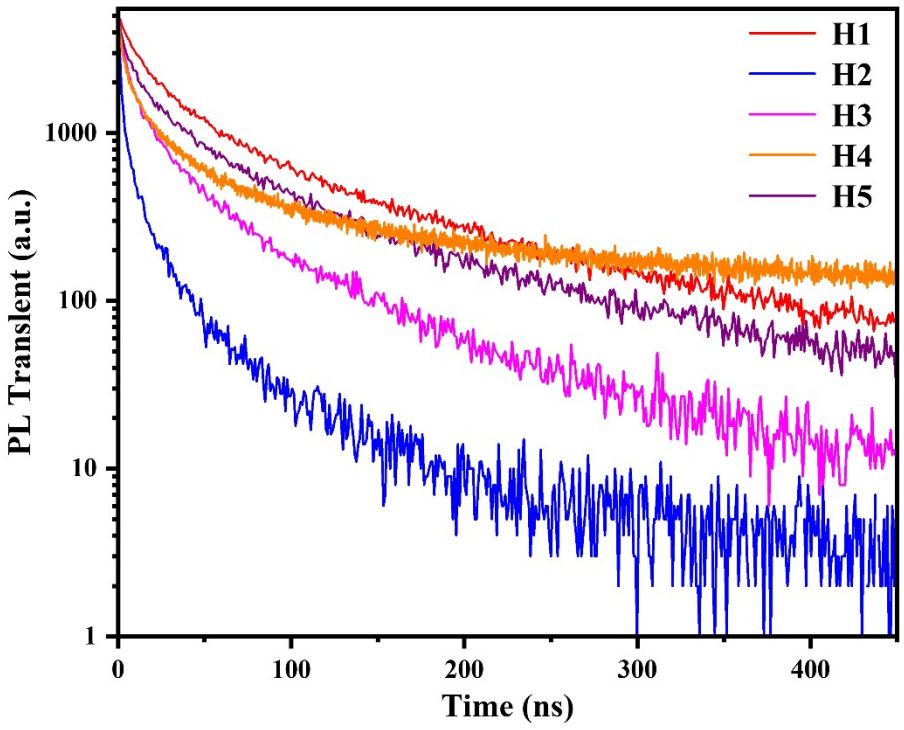

Figure S 11 Excited state lifetimes of H1-H5.

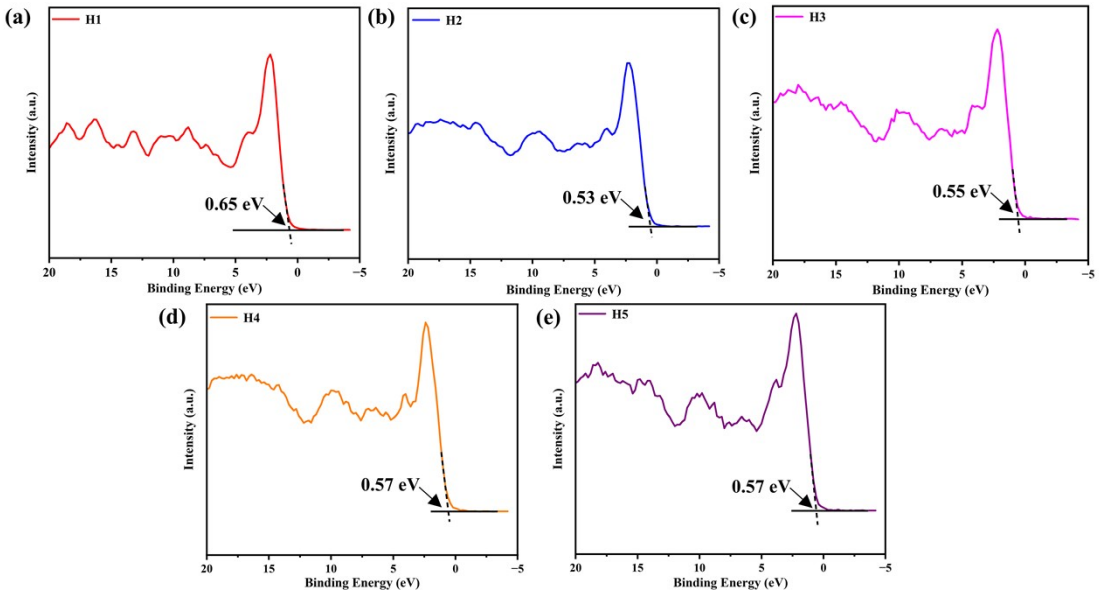

Figure S 12 (a)-(e) VB XPS results for H1-H5 and the valence band maxima (VBM) obtained through them.

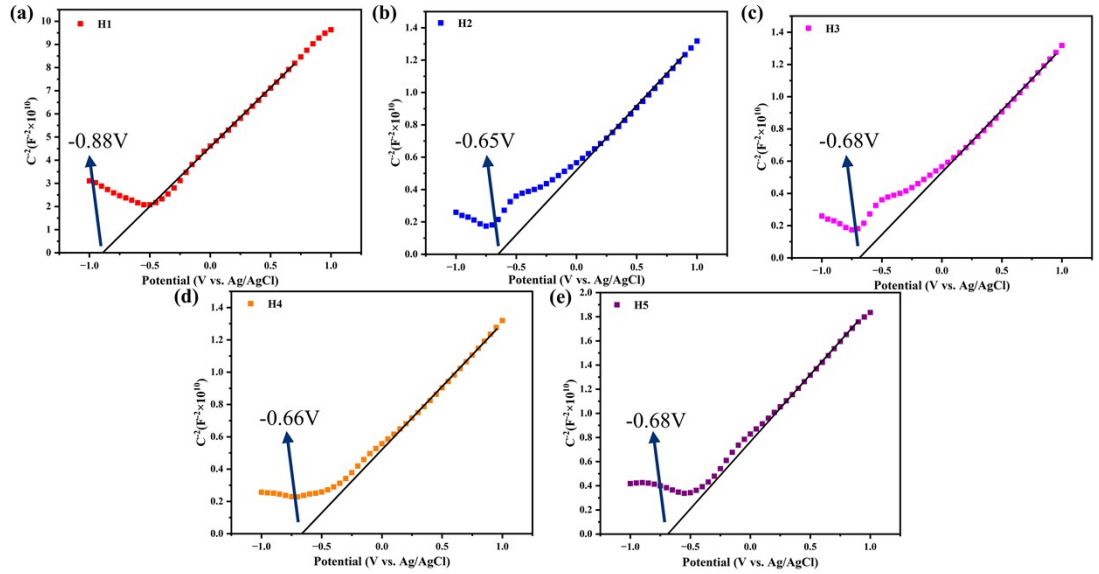

Figure S 13 Determination of the Mott Schottky curves for H1-H5 and the resulting conduction band minimum (CBM). (Mott Schottky curves are measured using a solution of dispersed solids coated on an electrode)

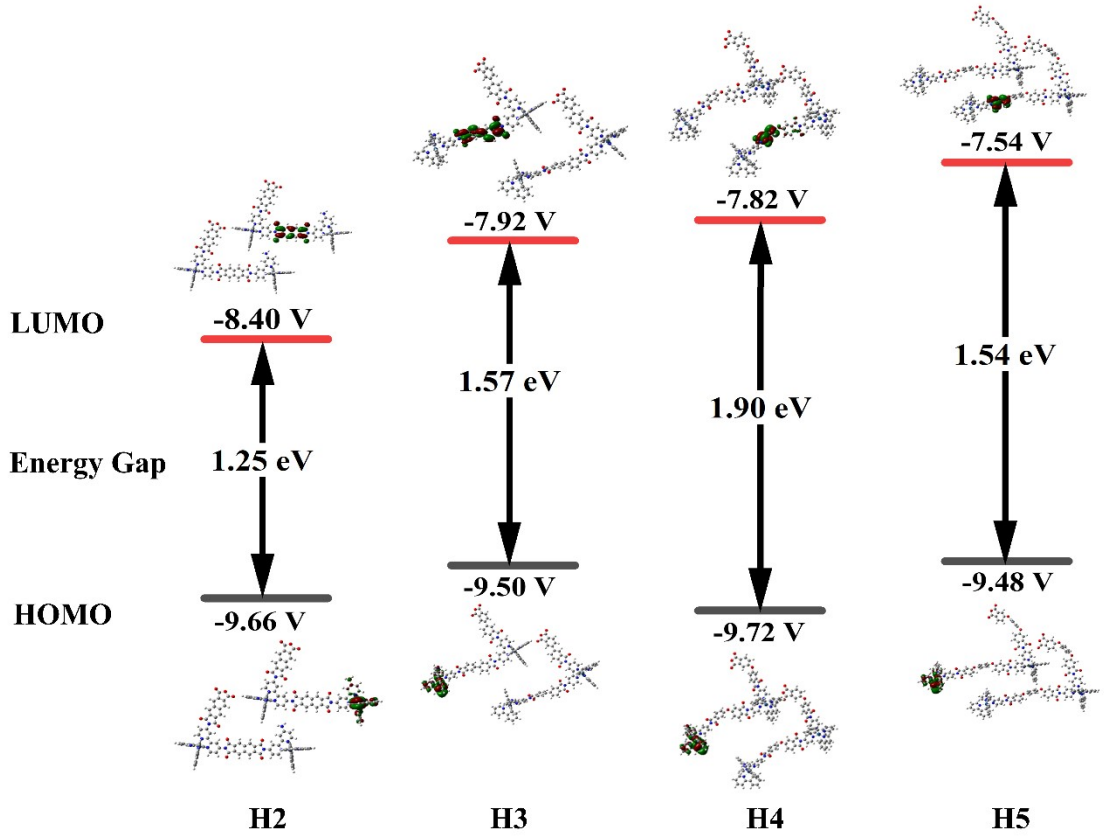

Figure S 14 Energy levels, energy gaps (in eV), and contour plots of HOMO and LUMO for the horizontal stacked configuration of the H2-H5 bilayer.

For H2 and H3, when two molecules are superimposed in the same plane, HOMO and LUMO are located on H1 part and the anhydride linker part, respectively, which is the same as in the unimolecular state, indicating that the horizontal stacked state does not affect the front orbital distributions of H2 and H3. The calculated of the energy gap shows that H3 has a larger energy gap than H2. Unlike H2 and H3, the distribution of the front orbitals of H4 and H5 is different from the unimolecular state. In the horizontal stacked state, the HOMO of H4 and H5 are located on the H1 within one molecule and LUMO of H4 and H5 are located on the anhydride linker within the other oligomer molecule, respectively. And the energy gap of H5 is lower than that of H4 (Figure S14). HOMO and LUMO of H4 and H5 are located on two molecules in

the superposition, providing an intermolecular transfer process for the electron transfer.

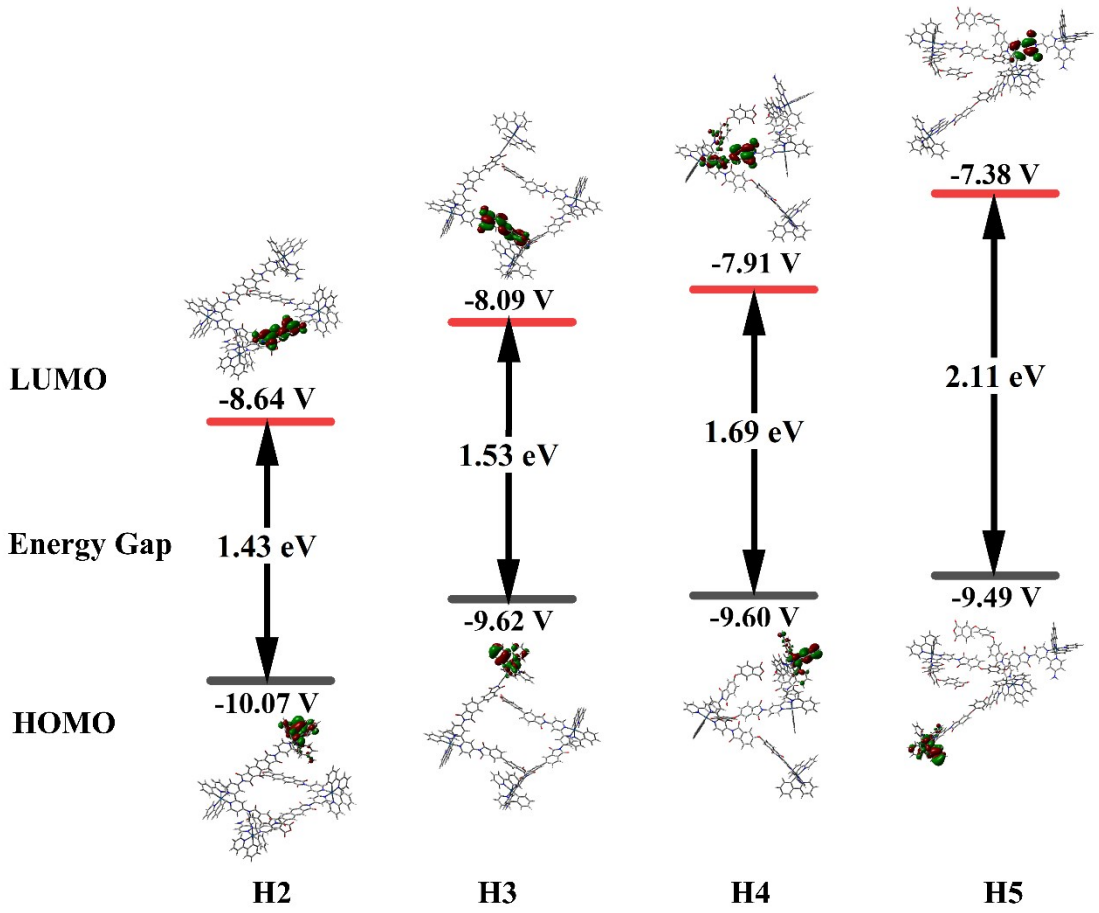

Figure S 15 Energy levels, energy gaps (in eV), and contour plots of HOMO and LUMO for the vertical crossed configuration of the H2-H5 bilayer.

When the two molecules cross vertically, the HOMO and LUMO of H3 are located in the H1 portion and the anhydride linker portion, respectively, which is the same as in the unimolecular state, suggesting that this conformation does not affect the distribution of the front orbitals of H3. Unlike H3, the HOMOs of H2, H4 and H5 are located on H1 within one molecule and the LUMOs are located on the anhydride linker within the other oligomer molecule. The LUMOs of H4 are more specifically distributed on both molecules. Such a distribution of the front orbitals provides an intermolecular transfer

process for electron transfer. In terms of energy gap changes, the band gap in the vertically crossed state agrees with the calculations for a single molecule, with a gradual increase from H2 to H5.

Table S3 Bimolecular binding energies (the energy of dimer minus 2 times of the energy of single molecule) of H1-based oligomers in different stacking states

	Planar Superposition (eV)	Vertical Cross (eV)	Vertically Stacked (eV)
H2	2.57	3.41	2.28
H3	2.32	2.28	1.82
H4	2.42	2.21	2.13
H5	2.75	2.69	2.46

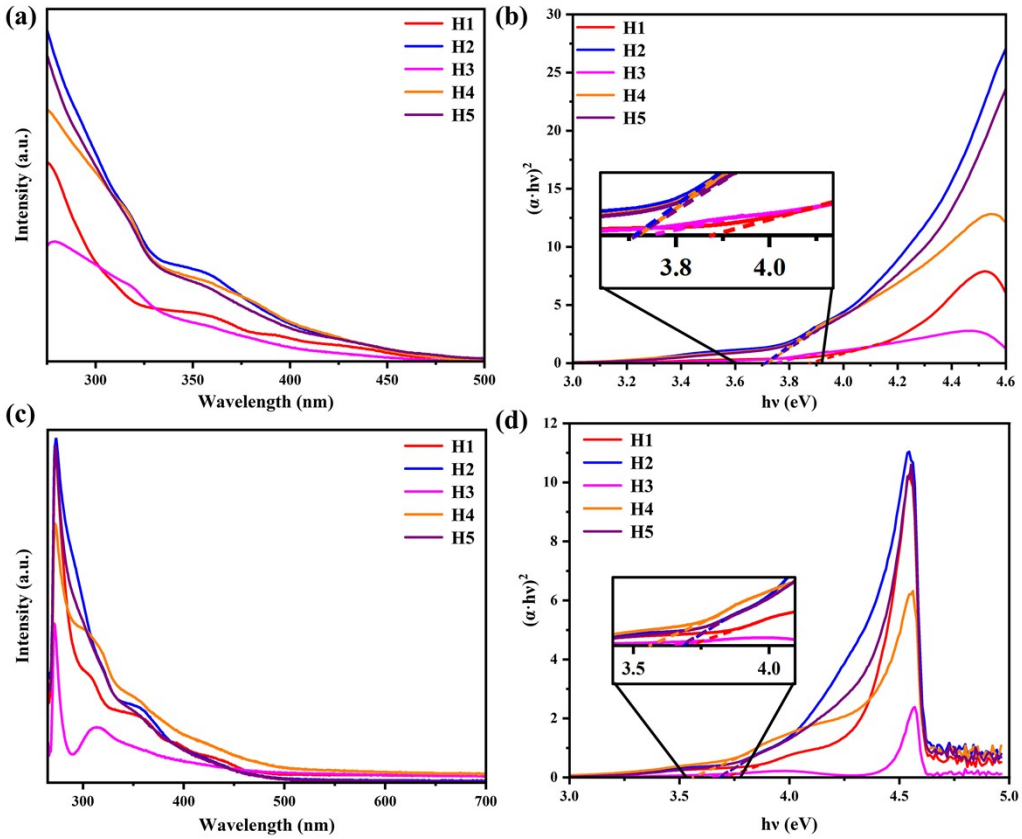

Figure S 16 (a)-(b) UV absorption spectra of 0.001 g/L of H1-H5 in DMF/H_2O/TEA (3/1/1, v/v/v), and energy gaps obtained by Tauc plots. (c)-(d) UV absorption spectra of 0.001 g/L of H1-H5 in DMF/TEA (3/1, v/v), and energy gaps obtained by Tauc plots.

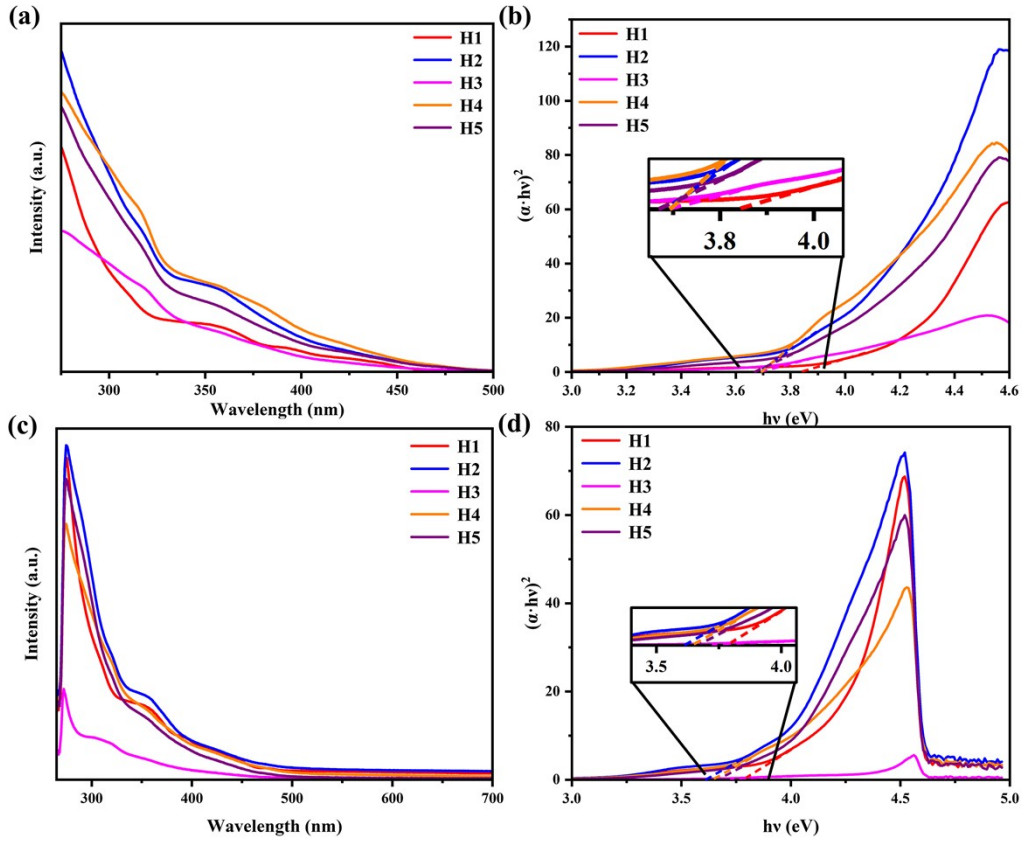

Figure S 17 (a)-(b) UV absorption spectra of 0.025 g/L of H1-H5 in DMF/H_2O/TEA (3/1/1, v/v/v), and energy gaps obtained by Tauc plots. (c)-(d) UV absorption spectra of 0.025 g/L of H1-H5 in DMF/TEA (3/1, v/v), and energy gaps obtained by Tauc plots.

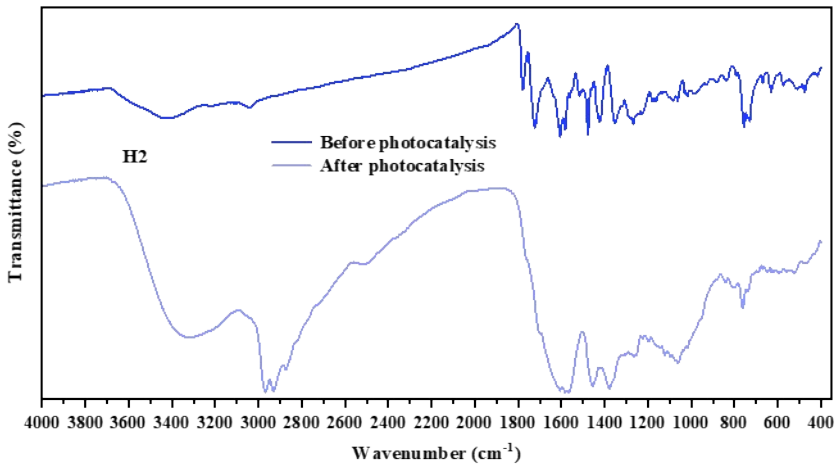

Figure S 18 FT-IR spectra before and after H2 photocatalysis.

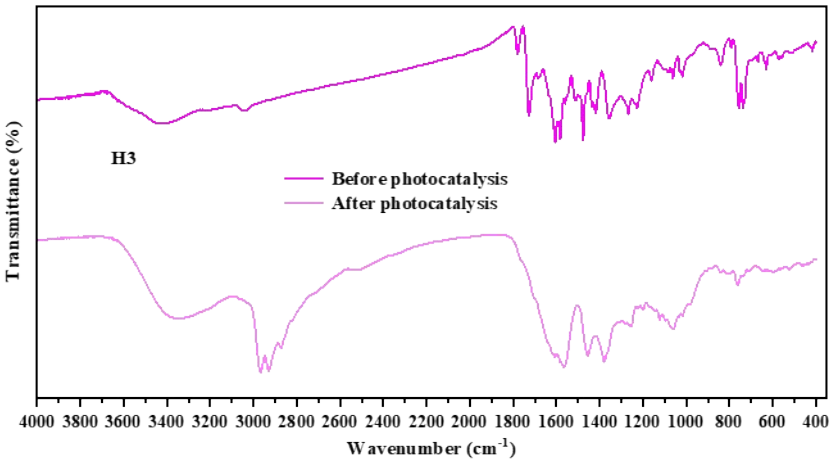

Figure S 19 FT-IR spectra before and after H3 photocatalysis.

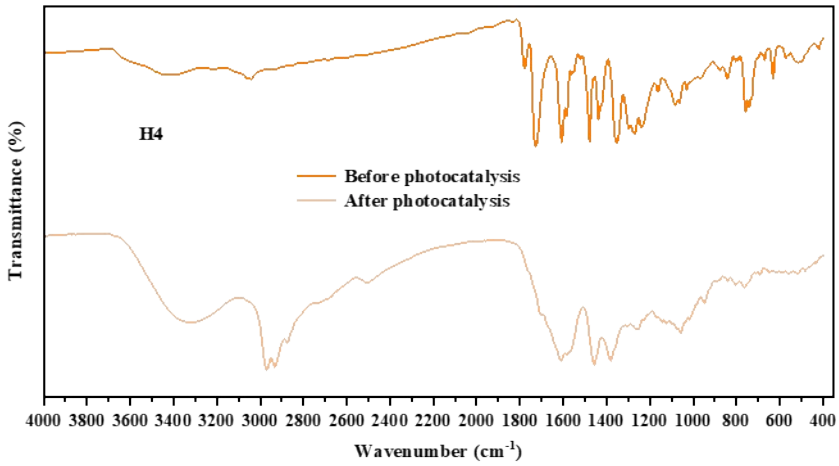

Figure S 20 FT-IR spectra before and after H4 photocatalysis.

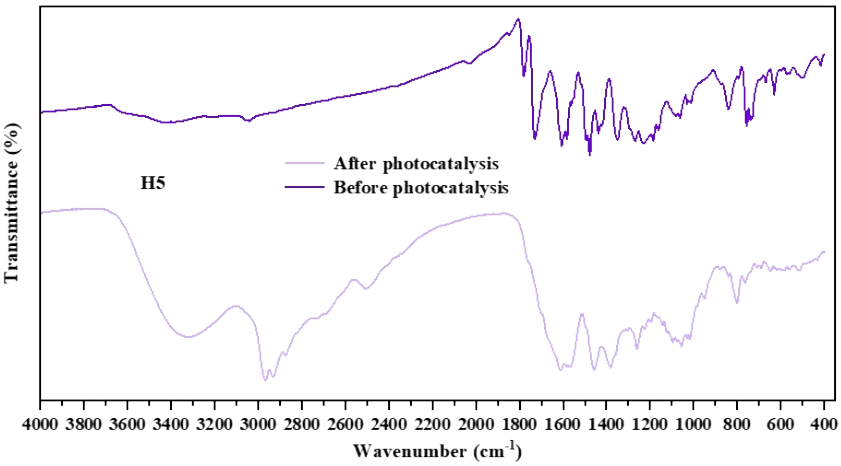

Figure S 21 FT-IR spectra before and after H5 photocatalysis.

According to the comparative results of FT-IR, after photocatalysis, even after evaporation of the solvent under reduced pressure, extremely distinct solvent peaks were still present in the spectra, suggesting that the organic solvent molecules may

combine with the photosensitizer to form solvated structures. It can be inferred from the merged peak at the imine position that the imine structure is still retained. These indicate that the molecular chain of the oligomer is more stable.

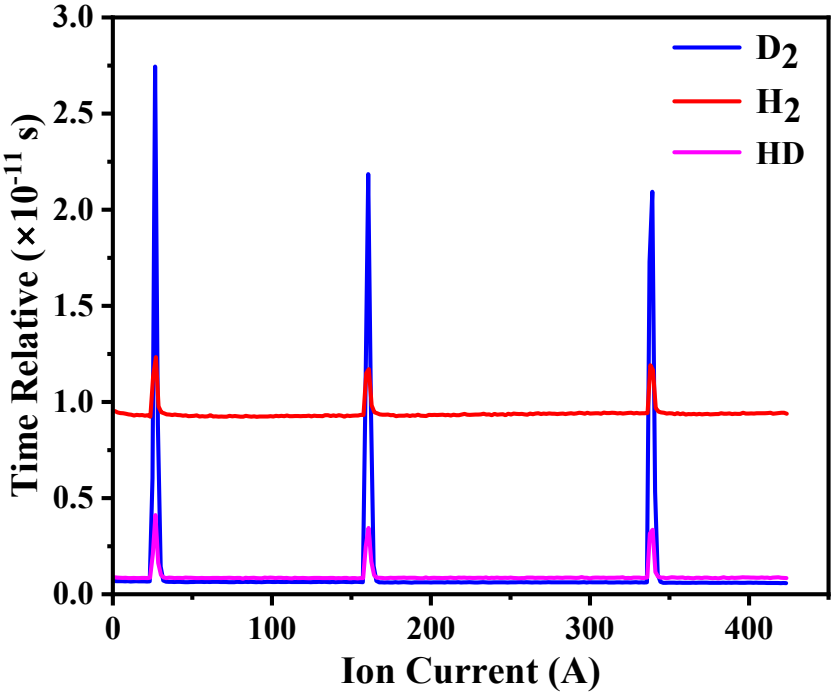

Figure S 22 The isotopic tracer assay results for H4.

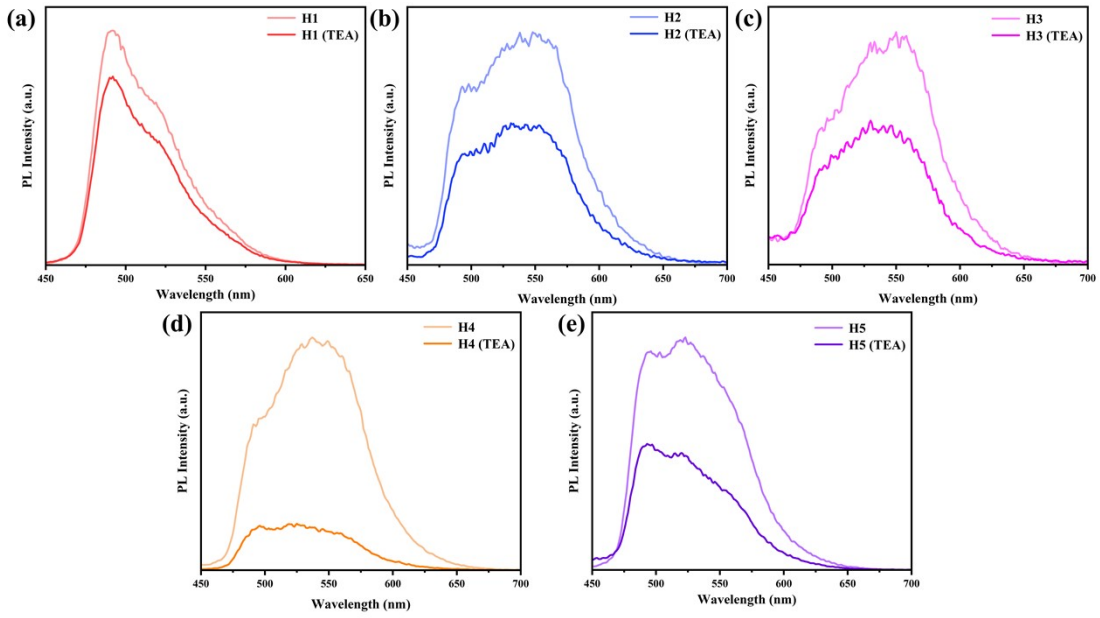

Figure S 23 Fluorescence quenching experiments of H1-H5.

References

1. M. J. Frisch, G. W. Trucks, H. B. Schlegel, G. E. Scuseria, M. A. Robb, J. R. Cheeseman, G. Scalmani, V. Barone, B. Mennucci, G. A. Petersson, H. Nakatsuji, M. Caricato, X. Li, H. P. Hratchian, A. F. Izmaylov, J. Bloino, G. Zheng, J. L. Sonnenberg, M. Hada, M. Ehara, K. Toyota, R. Fukuda, J. Hasegawa, M. Ishida, T. Nakajima, Y. Honda, O. Kitao, H. Nakai, T. Vreven, J. A. Montgomery Jr., J. E. Peralta, F. Ogliaro, M. Bearpark, J. J. Heyd, E. Brothers, K. N. Kudin, V. N. Staroverov, T. Keith, R. Kobayashi, J. Normand, K. Raghavachari, A. Rendell, J. C. Burant, S. S. Iyengar, J. Tomasi, M. Cossi, N. Rega, J. M. Millam, M. Klene, J. E. Knox, J. B. Cross, V. Bakken, C. Adamo, J. Jaramillo, R. Gomperts, R. E. Stratmann, O. Yazyev, A. J. Austin, R. Cammi, C. Pomelli, J. W. Ochterski, R. L. Martin, K. Morokuma, V. G. Zakrzewski, G. A. Voth, P. Salvador, J. J. Dannenberg, S. Dapprich, A. D. Daniels, O. Farkas, J. B. Foresman, J. V. Ortiz, J. Cioslowski and D. Fox, J. Gaussian 09, Revision B.01, Gaussian, Inc., Wallingford, CT, 2010.
2. E. Runge and E. K. U. Gross, Phys. Rev. Lett., 1984, 52, 997.
3. Becker, A. D. J. Chem. Phys. 1993, 98, 1372.
4. Lee, C.; Yang, W.; Parr, R. G. Phys. ReV. B 1988, 37, 785.
5. P. J. Hay and W. R. Wadt, J. Chem. Phys., 1985, 82, 270.
6. P. J. Hay and W. R. Wadt, J. Chem. Phys., 1985, 82, 299.